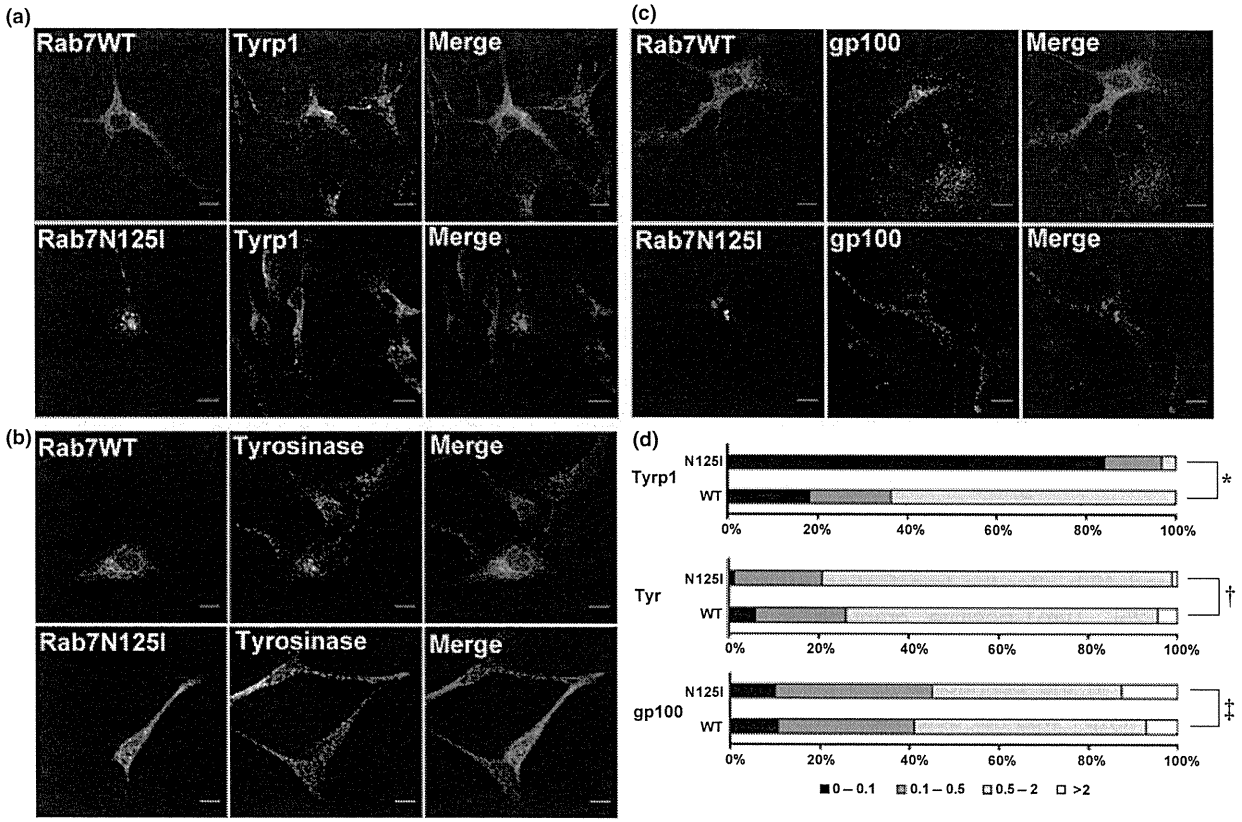

Figure 3. Rab7N125I eliminated Tyrp1, but not tyrosinase or gp100. Melan-A cells transfected with the plasmid encoding Rab7WT (a–c, upper panels) or Rab7N125I (a–c, lower panels) were immunostained with the anti-flag antibody (a–c, left) and antibody against melanosomal proteins, anti-Tyrp1 (a, middle), anti-tyrosinase (b, middle) or anti-gp100 (c, middle) antibodies. Merged images are shown on the right. Scale bars = 10 μm. (d) Tyrp1-specific elimination was statistically verified. Fifty-five to seventy-five images of Rab7WT- or Rab7N125I-expressing cells were randomly collected from each immunostaining experiment and were categorized into four types according to the relative intensity of Tyrp1, tyrosinase or gp100 immunostaining against that in surrounding control cells: 0–0.1, 0.1–0.5, 0.5–2 and >2. Bars are percentages of the cells in each category. $^{*}P < 0.0001$; $^{\dagger}P = 0.29$; $^{\ddagger}P = 0.73$. WT, Rab7WT-expressing cells; N125I, Rab7N125I-expressing cells.

DISCUSSION

In this study, we found that: (i) endogenous Tyrp1 was co-localized with Rab7 in the perinuclear areas in Rab7WT-expressing non-tumorigenic melanocytes; (ii) Tyrp1 was, in the dominant-negative Rab7-expressing cell, gradually eliminated by 48 h after transfection while tyrosinase and gp100 were not; and (iii) the elimination of Tyrp1 was partially rescued in the presence of proteasome inhibitor MG132. Importantly, only a small number of Tyrp1-positive vesicles were detected in the perinuclear area at 24 h after the transfection of mutant Rab7. Further 24 h incubation led to the complete elimination of Tyrp1. On the other hand, the signal intensities of tyrosinase and gp100 were not altered. These results suggest that Rab7 is more significantly involved in the trafficking of Tyrp1 to melanosomes than that of tyrosinase and gp100. It is conceivable that Tyrp1 traffics through endosomal compartments because Rab7 regulates maturation of early endosomes. The perinuclear Tyrp1-positive granules observed 24 h after the transfection of Rab7 mutants seemed to be endosomal structures. Similar Tyrp1 mislocalization was also observed in the earlier report by Hirosaki *et al.*[31] However, the reduction or elimination of Tyrp1 had never been observed. This discrepancy seems to derive from the different experimental approaches.

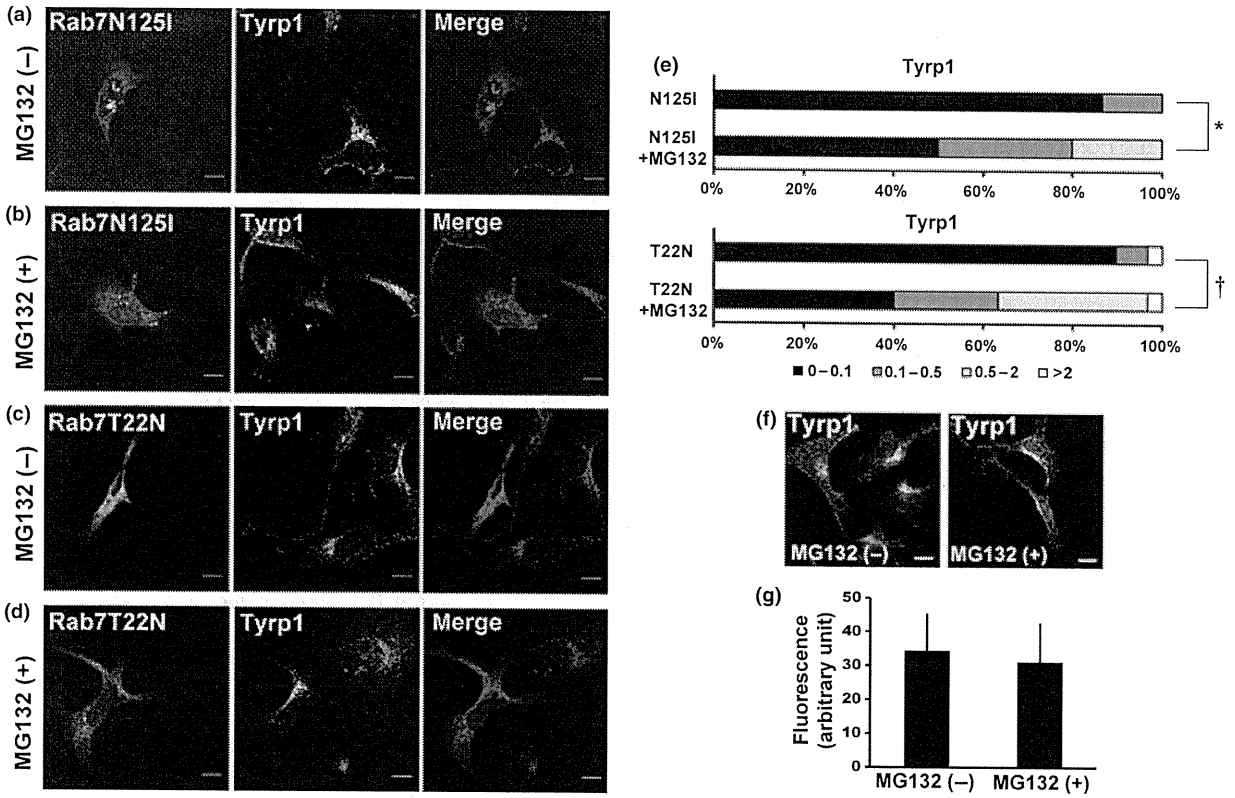

Figure 4. Proteasomal inhibitor MG132 partially rescued the Tyrp1 in mutant Rab7-expressing cells. Melan-A melanocytes were transfected with the plasmids encoding Rab7N125I (a,b) or Rab7T22N (c,d), and incubated for 48 h. Before fixation, cells were incubated in the absence (a,c) or presence (b,d) of 10 μmol/L MG132 for 5 h. Cells were immunostained with anti-flag and anti-Tyrp1 antibodies. Scale bars = 10 μm. (e) The rescue of Tyrp1 was statistically verified. Thirty cells expressing Rab7N125 and 30 cells expressing Rab7T22N in the presence of MG132 were compared with the same number of the cells expressing Rab7N125I and Rab7T22N in the absence of MG132, respectively. They were categorized into four types according to the relative intensity of Tyrp1 immunostaining to that in surrounding control cells: 0–0.1, 0.1–0.5, 0.5–2 and >2. Bars are the percentages of each cell pattern. $^{*}P = 0.0043$, $^{\dagger}P = 0.00046$. (f) Melan-A cells incubated with or without 10 μmol/L MG132 for 5 h were immunostained with anti-Tyrp1 antibody. Scale bars = 10 μm. (g) Graph shows fluorescence intensity of Tyrp1 in Melan-A cells measured from confocal images. Data are reported as means ± standard deviation.

Our results reflect a more physiological state than the previous ones: we observed endogenous Tyrp1 in non-tumorigenic melanocytes (not melanoma or non-melanocytic cells into which exogenous Tyrp1 was introduced). This also enabled us to examine the fate of endogenous Tyrp1 at the different time points after the Rab7 inhibition.

The differential sorting of melanosomal proteins and the Tyrp1-specific mislocalization/degradation have recently been studied. Biogenesis of lysosome-related organelles complex (BLOC)-1 and BLOC-2 play important roles in the transport of Tyrp1 from early endosomal structures to melanosomes. In melanocytes that lack one of the subunits of BLOC-1, Tyrp1 is mislocalized to early endosomes and the cell surface membrane, whereas the transport of tyrosinase and gp100 is not disrupted.[39] Tyrp1 is also reduced in BLOC-2-deficient melanocytes in mice and humans.[39,40] BLOC-1 appears to promote the exit of Tyrp1 from early endosomal membranes to another intermediate organelle from which BLOC-2 facilitates fusion with melanosomes.[41] On the other hand, AP also have important roles in the sorting of tyrosinase and Tyrp1. While AP-1 and AP-3 have some redundancy in the transport of tyrosinase, AP-1 seems to have a critical role in sorting Tyrp-1.[2,16,42] Considering these reports, AP-1, BLOC-1 and BLOC-2 seem to be involved in Tyrp1-specific

transport. The similar outcome caused by dysfunction of Rab7, AP-1 or BLOC suggests a close relationship of Rab7 with these complexes, though our results cannot specify whether Rab7 directly interacts with these complexes.

How was Tyrp1 eliminated after the Rab7 inhibition? MG132 partially rescued the Tyrp1 elimination, which suggests that Tyrp1 was eliminated by protein degradation machinery. MG132 inhibits not only proteasomal activities but lysosomal enzymes such as cathepsin B.[38] The dysfunction of BLOC results in Tyrp1 retention in the endosomal pathway and subsequent degradation in lysosomes.[39] Rab7 dysfunction may also result in the mislocalization and degradation of Tyrp1 in lysosomes. Another possibility is that Tyrp1 is directly degraded by the proteasomal pathway as suggested in growth hormone receptor degradation,[43] but the details of this degradation pathway remain unclear. These hypotheses need further examination in studies using lysosomal protease inhibitors. Furthermore, additional studies are needed to clarify how Tyrp1 promotes melanogenesis in the presence of Rab7 through the interaction with tyrosinase and gp100. Our previous studies indicated that the GTP-bound form of Rab7 promotes melanogenesis through the regulation of gp100 maturation in human melanoma cells.[34]

ACKNOWLEDGMENTS

We are grateful to Dorothy C. Bennett for providing the Melan-A cells and to Vincent J. Hearing for providing the PEP7.

REFERENCES

1 Dell'Angelica EC, Mullins C, Caplan S, Bonifacino JS. Lysosome-related organelles. *FASEB J* 2000; **14**: 1265–1278.
2 Raposo G, Tenza D, Murphy DM, Berson JF, Marks MS. Distinct protein sorting and localization to premelanosomes, melanosomes, and lysosomes in pigmented melanocytic cells. *J Cell Biol* 2001; **152**: 809–824.
3 Theos AC, Truschel ST, Raposo G, Marks MS. The Silver locus product Pmel17/gp100/Silv/ME20: controversial in name and in function. *Pigment Cell Res* 2005; **18**: 322–336.
4 Ito S, Wakamatsu K. Chemistry of mixed melanogenesis–pivotal roles of dopaquinone. *Photochem Photobiol* 2008; **84**: 582–592.
5 Cooksey CJ, Garratt PJ, Land EJ *et al.* Evidence of the indirect formation of the catecholic intermediate substrate responsible for the autoactivation kinetics of tyrosinase. *J Biol Chem* 1997; **272**: 26226–26235.
6 Kobayashi T, Urabe K, Winder A *et al.* Tyrosinase related protein 1 (TRP1) functions as a DHICA oxidase in melanin biosynthesis. *EMBO J* 1994; **13**: 5818–5825.
7 Kobayashi T, Hearing VJ. Direct interaction of tyrosinase with Tyrp1 to form heterodimeric complexes in vivo. *J Cell Sci* 2007; **120**: 4261–4268.
8 Boissy RE, Zhao H, Oetting WS *et al.* Mutation in and lack of expression of tyrosinase-related protein-1 (TRP-1) in melanocytes from an individual with brown oculocutaneous albinism: a new subtype of albinism classified as "OCA3". *Am J Hum Genet* 1996; **58**: 1145–1156.
9 Tomita Y, Takeda A, Okinaga S, Tagami H, Shibahara S. Human oculocutaneous albinism caused by single base insertion in the tyrosinase gene. *Biochem Biophys Res Commun* 1989; **164**: 990–996.
10 Hoashi T, Muller J, Vieira WD *et al.* The repeat domain of the melanosomal matrix protein PMEL17/GP100 is required for the formation of organellar fibers. *J Biol Chem* 2006; **281**: 21198–21208.
11 Wei ML. Hermansky-Pudlak syndrome: a disease of protein trafficking and organelle function. *Pigment Cell Res* 2006; **19**: 19–42.
12 Raposo G, Marks MS. Melanosomes–dark organelles enlighten endosomal membrane transport. *Nat Rev Mol Cell Biol* 2007; **8**: 786–797.
13 Calvo PA, Frank DW, Bieler BM, Berson JF, Marks MS. A cytoplasmic sequence in human tyrosinase defines a second class of di-leucine-based sorting signals for late endosomal and lysosomal delivery. *J Biol Chem* 1999; **274**: 12780–12789.
14 Huizing M, Sarangarajan R, Strovel E, Zhao Y, Gahl WA, Boissy RE. AP-3 mediates tyrosinase but not TRP-1 trafficking in human melanocytes. *Mol Biol Cell* 2001; **12**: 2075–2085.
15 Dell'Angelica EC, Shotelersuk V, Aguilar RC, Gahl WA, Bonifacino JS. Altered trafficking of lysosomal proteins in Hermansky-Pudlak syndrome due to mutations in the beta 3A subunit of the AP-3 adaptor. *Mol Cell* 1999; **3**: 11–21.
16 Theos AC, Tenza D, Martina JA *et al.* Functions of adaptor protein (AP)-3 and AP-1 in tyrosinase sorting from endosomes to melanosomes. *Mol Biol Cell* 2005; **16**: 5356–5372.
17 Bucci C, Thomsen P, Nicoziani P, McCarthy J, van Deurs B. Rab7: a key to lysosome biogenesis. *Mol Biol Cell* 2000; **11**: 467–480.
18 Gutierrez MG, Munafo DB, Beron W, Colombo MI. Rab7 is required for the normal progression of the autophagic pathway in mammalian cells. *J Cell Sci* 2004; **117**: 2687–2697.
19 Press B, Feng Y, Hoflack B, Wandinger-Ness A. Mutant Rab7 causes the accumulation of cathepsin D and

cation-independent mannose 6-phosphate receptor in an early endocytic compartment. *J Cell Biol* 1998; **140**: 1075–1089.
20 Vieira OV, Bucci C, Harrison RE *et al.* Modulation of Rab5 and Rab7 recruitment to phagosomes by phosphatidylinositol 3-kinase. *Mol Cell Biol* 2003; **23**: 2501–2514.
21 Bucci C, Chiariello M, Lattero D, Maiorano M, Bruni CB. Interaction cloning and characterization of the cDNA encoding the human prenylated rab acceptor (PRA1). *Biochem Biophys Res Commun* 1999; **258**: 657–662.
22 Cantalupo G, Alifano P, Roberti V, Bruni CB, Bucci C. Rab-interacting lysosomal protein (RILP): the Rab7 effector required for transport to lysosomes. *EMBO J* 2001; **20**: 683–693.
23 Dong J, Chen W, Welford A, Wandinger-Ness A. The proteasome alpha-subunit XAPC7 interacts specifically with Rab7 and late endosomes. *J Biol Chem* 2004; **279**: 21334–22142.
24 Johansson M, Olkkonen VM. Assays for interaction between Rab7 and oxysterol binding protein related protein 1L (ORP1L). *Methods Enzymol* 2005; **403**: 743–758.
25 Jordens I, Fernandez-Borja M, Marsman M *et al.* The Rab7 effector protein RILP controls lysosomal transport by inducing the recruitment of dynein-dynactin motors. *Curr Biol* 2001; **11**: 1680–1685.
26 Mizuno K, Kitamura A, Sasaki T. Rabring7, a novel Rab7 target protein with a RING finger motif. *Mol Biol Cell* 2003; **14**: 3741–3752.
27 Nakada-Tsukui K, Saito-Nakano Y, Ali V, Nozaki T. A retromerlike complex is a novel Rab7 effector that is involved in the transport of the virulence factor cysteine protease in the enteric protozoan parasite Entamoeba histolytica. *Mol Biol Cell* 2005; **16**: 5294–5303.
28 Stein MP, Feng Y, Cooper KL, Welford AM, Wandinger-Ness A. Human VPS34 and p150 are Rab7 interacting partners. *Traffic* 2003; **4**: 754–771.
29 Sun Y, Buki KG, Ettala O, Vaaraniemi JP, Vaananen HK. Possible role of direct Rac1-Rab7 interaction in ruffled border formation of osteoclasts. *J Biol Chem* 2005; **280**: 32356–32361.
30 Gomez PF, Luo D, Hirosaki K *et al.* Identification of rab7 as a melanosome-associated protein involved in the intracellular transport of tyrosinase-related protein 1. *J Invest Dermatol* 2001; **117**: 81–90.
31 Hirosaki K, Yamashita T, Wada I, Jin HY, Jimbow K. Tyrosinase and tyrosinase-related protein 1 require Rab7 for their intracellular transport. *J Invest Dermatol* 2002; **119**: 475–480.
32 Feng Y, Press B, Wandinger-Ness A. Rab7: an important regulator of late endocytic membrane traffic. *J Cell Biol* 1995; **131**: 1435–1452.
33 Kammann M, Laufs J, Schell J, Gronenborn B. Rapid insertional mutagenesis of DNA by polymerase chain reaction (PCR). *Nucleic Acids Res* 1989; **17**: 5404.
34 Kawakami A, Sakane F, Imai S *et al.* Rab7 regulates maturation of melanosomal matrix protein gp100/Pmel17/Silv. *J Invest Dermatol* 2007; **128**: 143–150.
35 Der JE, Dixon WT, Jimbow K, Horikoshi T. A murine monoclonal antibody, MoAb HMSA-5, against a melanosomal component highly expressed in early stages, and common to normal and neoplastic melanocytes. *Br J Cancer* 1993; **67**: 47–57.
36 Alwan HA, van Zoelen EJ, van Leeuwen JE. Ligand-induced lysosomal epidermal growth factor receptor (EGFR) degradation is preceded by proteasome-dependent EGFR de-ubiquitination. *J Biol Chem* 2003; **278**: 35781–35790.
37 Ettenberg SA, Magnifico A, Cuello M *et al.* Cbl-b-dependent coordinated degradation of the epidermal growth factor receptor signaling complex. *J Biol Chem* 2001; **276**: 27677–27684.
38 Longva KE, Blystad FD, Stang E, Larsen AM, Johannessen LE, Madshus IH. Ubiquitination and proteasomal activity is required for transport of the EGF receptor to inner membranes of multivesicular bodies. *J Cell Biol* 2002; **156**: 843–854.
39 Setty SR, Tenza D, Truschel ST *et al.* BLOC-1 is required for cargo-specific sorting from vacuolar early endosomes toward lysosome-related organelles. *Mol Biol Cell* 2007; **18**: 768–780.
40 Helip-Wooley A, Westbroek W, Dorward HM *et al.* Improper trafficking of melanocyte-specific proteins in Hermansky-Pudlak syndrome type-5. *J Invest Dermatol* 2007; **127**: 1471–1478.
41 Setty SR, Tenza D, Sviderskaya EV, Bennett DC, Raposo G, Marks MS. Cell-specific ATP7A transport sustains copper-dependent tyrosinase activity in melanosomes. *Nature* 2008; **454**: 1142–1146.
42 Huizing M, Anikster Y, Fitzpatrick DL *et al.* Hermansky-Pudlak syndrome type 3 in Ashkenazi Jews and other non-Puerto Rican patients with hypopigmentation and platelet storage-pool deficiency. *Am J Hum Genet* 2001; **69**: 1022–1032.
43 Flores-Morales A, Greenhalgh CJ, Norstedt G, Rico-Bautista E. Negative regulation of growth hormone receptor signaling. *Mol Endocrinol* 2006; **20**: 241–253.

Kobe J. Med. Sci., Vol. 57, No. 1, pp. E11-E16, 2011

Polymorphisms of Glutathione S-Transferase in Skin Cancers in a Japanese Population

KOJI CHIYOMARU*, TOHRU NAGANO and CHIKAKO NISHIGORI

Division of Dermatology, Department of Internal Related,
Kobe University Graduate School of Medicine, Kobe, Japan.
7-5-2 Kusunoki-cho, Chuo-ku, Kobe, 650-0017, Japan.

Received 11 January 2011/ Accepted 17 January 2011

Key Words: Polymorphism; SNP; Skin cancer; Glutathione s-transferase

ABSTRACT

Variations in the Glutathione S-transferase (GST) supergene family have been reported to influence cancer susceptibility in Caucasian. However the genetic backgrounds and skin types are quite different between Caucasian and non-Caucasian. We therefore investigated the distribution of GST gene polymorphism in non-Caucasian population to ascertain the role of this polymorphism in skin carcinogenesis. One-hundred and fifteen patients with skin cancers and 92 controls who visited Kobe University Hospital between April 2004 and November 2010 were enrolled in this study. Genotype of GST gene was determined by using polymerase chain reaction-restriction fragments length polymorphism analysis. The frequencies of GSTM1 positive genotype were significantly higher in squamous cell carcinomas than those in controls (adjusted odds ratio = 3.09, 95% confidence interval 1.04 - 9.21). The polymorphism of GSTM1 locus could be an important factor in susceptibility to squamous cell carcinoma among Japanese population.

INTRODUCTION

Members of the Glutathione S-transferase (GST) supergene family, which consists of eight gene subfamilies (GSTA, GSTK, GSTM, GSTO, GSTP, GSTT, GSTZ and MGST), are known to protect against chemical toxins and carcinogens by catalyzing the conjugation of glutathione to electrophiles in substrate (1 - 3).

Certain genes within the GSTM and GSTT (GSTM1 and GSTT1) subfamilies exhibit deletion polymorphisms which have been involved in cancer susceptibility (2, 4). Genetic variations at the GSTM1 loci have been shown to alter the susceptibility to basal cell carcinoma (BCC), squamous cell carcinoma (SCC) and malignant melanoma in the United Kingdom (5). Recent additional studies have implicated polymorphisms status of GSTM1 and T1 as relevant for the development of nonmelanoma skin cancers (NMSC) among Caucasian population (6 - 8).

On the other hand, differences between ethnic populations were observed in published reports of meta-analysis studies concerning GST genotypes at risk of gastric cancer and acute leukemia (9, 10). Moreover there has been no report focusing on susceptibility to skin cancers among non Caucasian population.

Phone: +81-78-382-6134 Fax: +81-78-382-6149 E-mail: 079m855m@stu.kobe-u.ac.jp

In this study, we analyzed the relationship between polymorphisms of GST supergene families and skin cancers in non-Caucasian population, and proposed to establish a simple screening method of identifying the high risk group for skin cancers.

MATERIALS AND METHODS

Study population.

One-hundred and fifteen patients with skin cancers (mean age ± standard deviation (SD), 75.3 ± 10.6 years; age range, 43 - 95 years) who visited the dermatology clinic in Kobe University Hospital between April 2004 and November 2010 were enrolled in this study. Skin cancers included 20 actinic keratoses (AK), 41 BCC, 25 SCC and 29 Bowen's diseases (BD). Bowenoid type actinic keratoses were included in AK. Clinical diagnosis was confirmed by histopathological analysis in all cases. The control group consists of 92 age- and sex-matched non affected unrelated Japanese individuals (mean age ± SD, 65.7 ± 14.0 years; age range, 28 - 89 years) from the same area in Japan with slight fungal or bacterial infections, or seborrheic keratosis. (Table I)

Table I. Clinical characteristics and number of cases and controls

	Control	Actinic keratosis	Basal cell carcinoma	Squamous cell carcinoma	Bowen's disease
Male	49	6	22	12	11
Female	43	14	19	13	18
Total	92	20	41	25	29
Mean-age: year±SD	65.7 ± 14.0	79.8 ± 7.2	72.8 ± 11.4	79.0 ± 9.1	72.7 ± 11.1

SD, standard deviation

We handled these patients as anonymous samples about which nobody could know their personal information other than their genotypes. Written informed consent was also obtained from all participants. The Medical Ethics Committee of Kobe University approved this work that was conducted in accordance with the Declaration of Helsinki principles.

Identification of genotypes.

Genomic DNA was extracted from peripheral mononuclear cells using a Qiagen FlexiGene DNA kit (Qiagen, Tokyo, JAPAN) according to the manufacturers' protocols. The GSTM1 null or positive (includes A, B and AB) genotype and GSTP1 Ile/Ile, Ile/Val and Val/Val polymorphism were determined by PCR-restriction fragment length polymorphisms (RFLP) technique. GSTT1 null and expressing subjects were identified by using a PCR approach. Each sequence of the primers, restriction enzymes and details of genotyping were described elsewhere (3). In some cases, determination of allelic polymorphism in GSTM1 and P1, PCR product was purified by a Qiagen PCR purification kit and DNA direct sequences analysis was performed using Applied Biosystems Model 377A Automated DNA Sequencer (Applied Biosystems, Foster City, CA).

Statistical analysis.

For statistical analysis, we used SPSS for Windows, version 17.0 (SPSS Japan Inc.) to calculate the adjusted odds ratio (AOR) and 95% confidence interval (CI). All adjusted models included age and sex.

RESULTS

Polymorphisms of GSTM1, GSTP1 and GSTT1 and skin cancer risk.

The polymorphisms in GST supergene family, GSTM1, GSTP1 and GSTT1 were investigated for NMSC. Their genotype distributions in skin cancers and controls are shown in Table II. We found a significantly increased risk of squamous cell carcinomas was associated with GSTM1 positive genotype (AOR = 3.09, 95% CI 1.04 - 9.21).

Table II. Distribution of Glutathione S-transferase genotypes in skin cancer patients and controls

Genotype	Controls (%)	Actinic keratosis			Bowen's disease		
		Cases (%)	OR (95% CI)	AOR (95% CI)	Cases (%)	OR (95% CI)	AOR (95% CI)
GSTM1							
null	46 (50.0)	7 (35.0)	1.0 (-)	1.0 (-)	13 (44.8)	1.0 (-)	1.0 (-)
positive	46 (50.0)	13 (65.0)	1.86 (0.68-5.08)	1.75 (0.57-5.37)	16 (55.2)	1.23 (0.53-2.85)	1.12 (0.47-2.66)
GSTP1							
Val/Val + Val/Ile	26 (28.3)	3 (15.0)	1.0 (-)	1.0 (-)	7 (24.1)	1.0 (-)	1.0 (-)
Ile/Ile	66 (71.7)	17 (85.0)	2.23 (0.60-8.26)	1.77 (0.41-7.70)	22 (75.9)	1.24 (0.47-3.25)	1.15 (0.42-3.11)
GSTT1							
null	39 (42.4)	10 (50.0)	1.0 (-)	1.0 (-)	13 (44.8)	1.0 (-)	1.0 (-)
positive	53 (57.6)	10 (50.0)	0.74 (0.28-1.94)	0.88 (0.29-2.63)	16 (55.2)	0.91 (0.39-2.10)	0.95 (0.39-2.32)

Genotype	Controls (%)	Basal cell carcinoma			Squamous cell carcinoma		
		Cases (%)	OR (95% CI)	AOR (95% CI)	Cases (%)	OR (95% CI)	AOR (95% CI)
GSTM1							
null	46 (50.0)	21 (51.2)	1.0 (-)	1.0 (-)	6 (24.0)	1.0 (-)	1.0 (-)
positive	46 (50.0)	20 (48.8)	0.95 (0.46-1.99)	0.88 (0.41-1.90)	19 (76.0)	3.17 (1.16-8.65)	3.09 (1.04-9.21)
GSTP1							
Val/Val + Val/Ile	26 (28.3)	11 (26.8)	1.0 (-)	1.0 (-)	7 (28.0)	1.0 (-)	1.0 (-)
Ile/Ile	66 (71.7)	30 (73.2)	1.07 (0.47-2.46)	0.92 (0.39-2.18)	18 (72.0)	1.01 (0.38-2.71)	0.57 (0.18-1.78)
GSTT1							
null	39 (42.4)	22 (53.7)	1.0 (-)	1.0 (-)	9 (36.0)	1.0 (-)	1.0 (-)
positive	53 (57.6)	19 (46.3)	0.64 (0.30-1.33)	0.61 (0.28-1.34)	16 (64.0)	1.31 (0.52-3.27)	1.39 (0.51-3.84)

OR, odds ratio; CI, confidence interval; AOR, adjusted odds ratio

Polymorphisms of GSTM1, GSTP1 and GSTT1 risk of SCC on sun-exposed or less-exposed skin area.

To assess the effect of sun-exposure, we subdivided the SCCs whether the lesion was on the sun-exposed area or not (Table III). The GSTM1 positive genotype may be associated with SCC risk according to non-sun-exposed lesion (AOR = 5.79, 95% CI 1.15 - 29.1).

Table III. Distribution of Glutathione S-transferase in squamous cell carcinoma on sun-exposed or less-exposed skin area

Genotype	Controls (%)	SCC on sun-exposed area			SCC on less-exposed area		
		Cases (%)	OR (95% CI)	AOR (95% CI)	Cases (%)	OR (95% CI)	AOR (95% CI)
GSTM1							
null	46 (50.0)	4 (33.3)	1.0 (-)	1.0 (-)	2 (15.4)	1.0 (-)	1.0 (-)
positive	46 (50.0)	8 (66.7)	2.00 (0.56-7.11)	1.76 (0.43-7.12)	11 (84.6)	5.50 (1.16-26.2)	5.79 (1.15-29.1)
GSTP1							
Val/Val + Val/Ile	26 (28.3)	3 (25.0)	1.0 (-)	1.0 (-)	4 (30.8)	1.0 (-)	1.0 (-)
Ile/Ile	66 (71.7)	9 (75.0)	1.18 (0.30-4.71)	0.66 (0.13-3.32)	9 (69.2)	0.89 (0.25-3.13)	0.60 (0.15-2.37)
GSTT1							
null	39 (42.4)	6 (50.0)	1.0 (-)	1.0 (-)	3 (23.1)	1.0 (-)	1.0 (-)
positive	53 (57.6)	6 (50.0)	0.74 (0.22-2.46)	0.69 (0.18-2.67)	10 (76.9)	2.45 (0.63-9.51)	2.36 (0.58-9.66)

OR, odds ratio; CI, confidence interval; AOR, adjusted odds ratio

DISCUSSION

In our study, marked differences in the distribution of GSTM1 genotype were found between SCC and control (Table II). In addition, the frequency of homozygous deletions of GSTM1 was surprisingly reduced the risk of SCC on less-exposed area in Japanese population.

In general, GST null genotype is reported to susceptibility of skin cancer (7, 11-13), and also the enzymatic activity is lower than GST positive genotype (14, 15). On the view point of carcinogenesis, lower activity of GST enzymes is likely to induce cell damage that finally causes production of skin cancer.

GSTs detoxify reactive oxygen species (ROS) which can directly attack DNA and can cause DNA damage (11). UV exposure is one of the major factors involved in the process of skin carcinogenesis. UV generates ROS and oxidative DNA damage caused by UV is involved in skin carcinogenesis. Thus, it could be possible that insufficient function of GST might cause oxidative stress related skin cancers. In fact Carless et al. reported that the GSTM1 null genotype confers an increased risk for solar keratosis development in an Australian Caucasian population (6).

Nevertheless, our results did not indicate that null type of GST is involved in the susceptibility of AK or SCC on the sun-exposed area. Rather, SCCs on both sun-exposed skin area and less-exposed skin area were closely related to the GSTM1 positive genotypes (Table III).

The reason of these conflicting results is unknown. The difference in the acute sunburn inflammation among the ethnic group could be one of the reasons for this discrepancy. The studies of polymorphism in the susceptibility of carcinogenesis were sometimes competing. Different ethnic, racial, environmental factor and so on could be related to the results.

In Japanese population, GSTM1 null genotypes may be alter the enzymatic activity but induce another pathway of protecting cancer development, further analysis are needed.

Like that of the GSTM1 gene, GSTT1 also has a null genotype. According to the previous data, the null genotype was seen in approximately 20% of the cases and controls in the Caucasian population (6, 11). In our study the distributions of GSTT1 null genotype were quite different from the data among Caucasian population both in cases (48.9%) and controls (42.4%). The frequency of GSTT1 null type did not differ between patients and controls.

The homozygous variant genotype of GSTP1 (Val/Val) has been seen in other study to be involved in an increase in susceptibility of other cancer types. Although previous study indicated that polymorphism at the GSTP1 locus would be an important factor in susceptibility to bladder and testicular cancer (4), no significant difference in the frequencies of GSTP1 wild type (Ile/Ile) and variant types (Val/Val, Val/Ile) could be demonstrated between controls and skin cancer groups in our analysis. Since GSTM1 and T1 protect against oxidized lipid and oxidized DNA, epoxide, and cytotoxic reagents, individuals nulled at both GSTM1 and T1 loci would be expected to be at a greater risk than those lacking only one gene (16). In our study, there was no correlation between SCC susceptibility and null type of both GSTM1 and T1.

One possible explanation for our results is that GSTM1 positive phenotype suppresses cell apoptosis that might allow the survival of mutated cells, since GSTP1 suppresses cell apoptosis and over expression of GSTP1 is reported in many types of cancers (17). In addition there could be various other pathways through which other genes can act, in particular genes involved in cell cycle regulation, DNA repair and other anticancer immune mechanisms, these would be expected to act independently of GSTM1 pathway (18).

Since the number of the cases and controls in our study were insufficient, further studies should explore the association between GST gene polymorphisms and skin cancer susceptibility in non-Caucasian population.

In conclusion, the polymorphism at the GSTM1 locus could be an important factor in susceptibility to SCC in Japanese population. Therefore, a better understanding of the factors that predispose to the SCC will enable identification of causative factors and development of prevention strategies, especially identification of high risk group for SCC. High risk patients could be included into skin cancer surveillance program to promote earlier detection of SCC.

ACKNOWLEDGEMENTS

This study was partially supported by a grant from Global Center of Excellence for Education and Research on Signal Transduction Medicine in the Coming Generation.

REFERENCES

1. **Strange, R.C. and Fryer, A.A.** The glutathione S-transferase: influence of polymorphism on cancer susceptibility. In Boffetta, P., Caporaso, N., Cuzick, J., Lang, M., Vineis, P. eds. Metabolic polymorphisms and cancer. IARC Scientific Publications, IARC, Lyon, pp. 231-249.
2. **Zhong, S., Wyllie, A.H., Barnes, D., Wolf, C.R. and Spurr, N.K.** Relationship between the GSTM1 genetic polymorphism and susceptibility to bladder, breast and colon cancer. Carcinogenesis 1993; **14:** 1821-1824.
3. **Curran, J.E., Weinstein, S.R. and Griffiths, L.R.** Polymorphisms of glutathione S-transferase genes (GSTM1, GSTP1 and GSTT1) and breast cancer susceptibility. Cancer letters 2000; **153:** 113-120.
4. **Harries, L.W., Stubbins, M.J., Forman, D., Howard, G.C. and Wolf, C.R.** Identification of genetic polymorphisms at the glutathione S-transferase Pi locus and association with susceptibility to testicular, breast and prostate cancer. Carcinogenesis 1997; **18:** 641-644.
5. **Heagerty, A.H., Fitzgerald, D., Smith, A., Bowers, B., Jones, P., Fryer, A.A., Zhao, L., Alldersea, J. and Strange, R.C.** Glutathione S-transferase GSTM1 phenotypes and protection against cutaneous tumours. Lancet 1994; **343:** 266-268.
6. **Carless, M.A., Lea, R.A., Curran, J.E., Appleyard, B., Gaffney, P., Green, A. and Griffiths, L.R.** The GSTM1 null genotype confers an increased risk for solar keratosis development in an Australian Caucasian population. J Invest Dermatol 2002; **119:** 1373-1378.
7. **Ramsay, H.M., Harden, P.N., Reece, S., Smith, A.G., Jones, P.W., Strange, R.C. and Fryer, A.A.** Polymorphisms of glutathione S-transferase are associated with altered risk of nonmelanoma skin cancer in renal transplant recipients: A preliminary analysis. J Invest Dermatol 2001; **117:** 251-255.
8. **Fryer, A.A., Ramsay, H.M., Lovatt, T.J., Jones, P.W., Hawley, C.M., Nicol, D.L., Strange, R.C. and Harden, P.N.** Polymorphisms in glutathione S-transferase and non-melanoma skin cancer risk in Australian renal transplant recipients. Carcinogenesis 2005; **26:** 185-191.
9. **Ye, Z. and Song, H.** Glutathione S-transferase polymorphisms (GSTM1, GSTP1 and GSTT1) and the risk of acute leukemia: a systemic review and meta-analysis. Eur J Cancer 2005; **41:** 980-989.
10. **La Torre, G., Boccia, S. and Ricciardi, G.** Glutathione S-transferase M1 status and

gastric cancer risk: a meta-analysis. Cancer lett 2005; **217:** 53-60.

11. **Mossner, R., Andres, N., Konig, I.R., Kruger, U., Schmidt, D., Berking, C., Ziegler, A., Brockmoller, J., Kaiser, R., Volkenandt, M., Westphal, G.A. and Reich, K.** Variations of the melanocortin-1 receptor and the glutathione S-transferase T1 and M1 genes in cutaneous malignant melanoma. Arch Dermatol Res 2007; **298:** 371-379.
12. **Shanley, S.M., Chenevix-Trench, G., Palmer, J. and Hayward, N.** Glutathione S-transferase GSTM1 null type in Australian patients with nevoid bacal cell carcinoma syndrome or sporadic melanoma. Carcinogenesis 1995; **16:** 2003-2004.
13. **Lira, M.G., Provezza, L., Malerba, G., Naldi, L., Remuzzi, G., Boschiero, L., Forni, A., Rugiu, C., Piaserico, S., Alaibac, M., Turco, A., Girolomoni, G. and Tessari, G.** et al. Glutathione S-transferase and CYP1A1 gene polymorphisms and non-melanoma skin cancer risk in Italian transplanted patients. Exp Dermatol 2006; **15:** 958-965.
14. **Hayes, J.D. and Strange, R.C.** Glutathione S-transferase polymorphisms and their biological consequences. Pharmacology. 2000; **61:** 154-166.
15. **Stewart, R.K., Smith, G.B.J., Donnelly, P.J., Reid, K.R., Petsikas, D., Conlan, A.A. and Massey, T.E.** Glutathione S-transferase-catalyzed conjugation of bioactivated aflatoxin B1 in human lung: differential cellular distribution and lack of significance of the GSTM1 genetic polymorphism. Carcinogenesis. 1999; **20:** 1971-1977.
16. **Elexpuru-Camiruaga, J., Buxton, N., Kandula, V., Dias, P.S., Cambell, D., McIntosh, J., Broome, J., Jones, P., Inskip, A., Alldersea, J., Fryer, A.A. and Strange, R.C.** Susceptibility to astrocytoma and meningioma: Influence of alleism at glutathione S-transferase (GSTT1 and GSTM1) and Cytochrome p-450 (CYP2D6) loci. Cancer Res 1995; **55:** 4237-4239.
17. **Mutallip, M., Nohata, N., Hanazawa, T., Kikkawa, N., Horiguchi, S., Fujimura, L., Kawakami, K., Chiyomaru, T., Enokida, H., Nakagawa, M., Okamoto, Y. and Seki, N.** Glutathione S-transferase P1 (GSTP1) suppresses cell apoptosis and its regulation by miR-133α in head and neck squamous cell carcinoma (HNSCC). Int J Mol Med 2010; Epub ahead of print.
18. **Lear, J.T., Smith, A.G., Strange, R.C. and Fryer, A.A.** Detoxifying enzyme genotypes and susceptibility to cutaneous malignancy. Br J Dermatol 2000: **142:** 8-15.

BRIEF COMMUNICATION

Dysfunction of melanocytes in photoleukomelanoderma following photosensitivity caused by hydrochlorothiazide

Eriko Masuoka, Toshinori Bito, Hideki Shimizu & Chikako Nishigori

Division of Dermatology, Department of Internal Related, Kobe University Graduate School of Medicine, Kobe, Japan

Key words:
hydrochlorothiazide; leukomelanoderma; melanocyte; photosensitivity

Correspondence:
Dr Chikako Nishigori, MD, PhD, Division of Dermatology, Department of Internal Related, Kobe University Graduate School of Medicine, 7-5-2 Kusunoki-cho, Chuo-ku, Kobe 650 0017, Japan.
Tel: +81-78 382 6134
Fax: +81 78 382 6149
e-mail: chikako@med.kobe-u.ac.jp

Accepted for publication:
13 July 2011

Conflicts of interest:
None declared.

Summary

We report a 68-year-old Japanese man who developed photoleukomelanoderma following prolonged photosensitivity caused by hydrochlorothiazide. He showed complete recovery from the leukomelanoderma with the discontinuation of the responsive drug and with topical application of tacrolimus hydrate and corticosteroid. Histological and immunohistochemical examination revealed that there were no melanin-positive cells in the hypopigmented area, despite the presence of melanocytes. These results and the clinical course indicate that leukomelanoderma is postulated temporary dysfunction of melanocytes. We also conducted a review of previous case reports regarding drug-induced photoleukomelanoderma.

Photoleukomelanoderma is a rare condition in which the pathogenesis is not fully understood. It is thought that factors such as the intensity and duration of sunlight exposure, skin color and genetic background influence the development of photoleukomelanoderma (1). Here, we report a case of photoleukomelanoderma following prolonged photosensitivity caused by hydrochlorothiazide. The patient completely recovered from leukomelanoderma after discontinuation of the hydrochlorothiazide and topical application of tacrolimus and corticosteroid. Histological and immunohistochemical examination of a dyspigmented macula suggests that the condition was due to melanocyte dysfunction.

Case report

A 68-year-old Japanese man was referred to our hospital in February 2010 with a 6-month history of a skin rash on the sun-exposed areas. He had been taking losartan potassium/hydrochlorothiazide (Preminent®, MSD K. K., Tokyo, Japan; 50 mg of losartan potassium and 12.5 mg of hydrochlorothiazide per tablet) one tablet/day for 9 months for hypertension. A pruritic erythema developed on the sun-exposed areas 3 months after commencing Preminent®. His past history included brain infarction, angina pectoris, and chronic hepatitis C. He had no past history of skin disease including photosensitive disorders.

On physical examination, erythematous brown-pigmented maculae were intermingled with hypopigmented maculae on his face, ears, neck, and on the dorsa of his hands (Fig. 1a, b). Laboratory examinations including complete blood count and liver and renal function showed no abnormal findings. Histological findings of the lesion encompassing hyperpigmented macula and hypopigmented macula from the dorsum of the right hand revealed hyperkeratosis, intra- and inter-cellular edema, liquefaction and acanthosis-like 'saw-toothing' of the rete ridges in the epidermis, together with inflammatory cell infiltration and some melanophages around capillaries in the upper dermis (Fig. 2a, c). Fontana–Masson stain showed an increase of melanin-positive cells in both the epidermis and dermis of the hyperpigmented lesion. In contrast, no positive cells were seen in the hypopigmented lesion (Fig. 2b, d); however, melanocytes with S-100 protein were observed even in the hypopigmented area (Fig. 2e). The minimal response dose (MRD) to ultraviolet (UV) A and minimal erythema dose (MED) to UVB were 6 J/cm^2 and 100 mJ/cm^2, respectively (Toshiba FL 32S BL and FL 32S E-30 lamps, Toshiba Electric Co., Tokyo, Japan), indicating photosensitivity to UVA. A photo-patch test with 30% Preminent® in

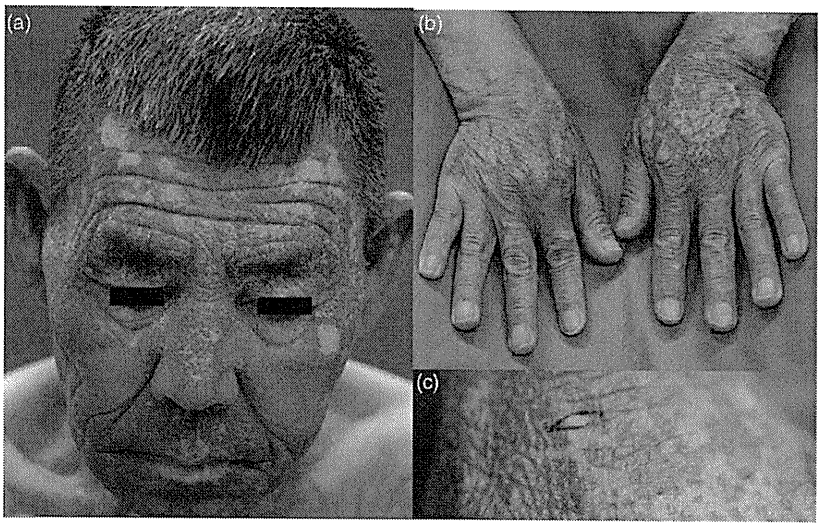

Fig. 1. (a) Dark brown pigmentation accompanied by pinkish hypopigmented spots was seen on the face, ears and neck. (b) Dark brown lichenificated plaques of various sizes were observed on the dorsa of the hands, and there were also areas of hypopigmentation. (c) A skin biopsy specimen was taken from the hand lesion encompassing both hyperpigmented and hypopigmented areas.

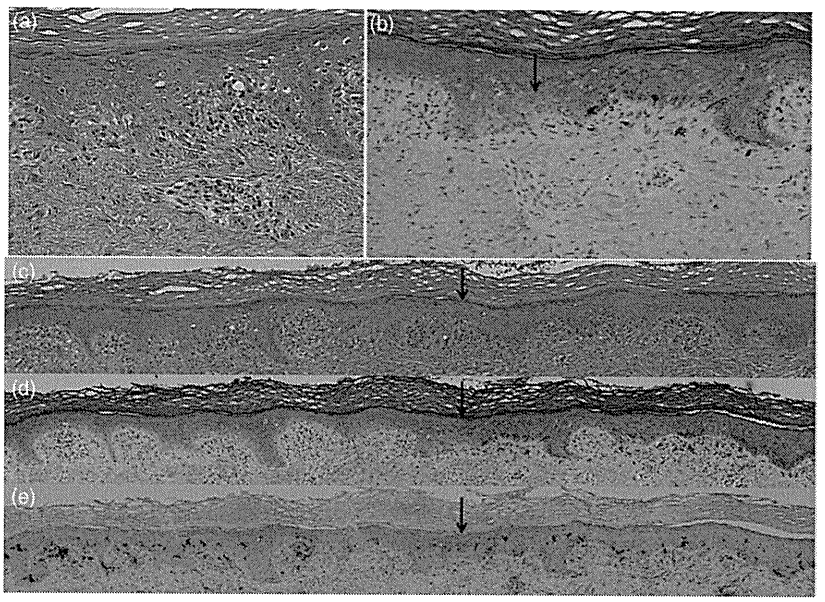

Fig. 2. (a) A specimen taken from the dorsum of his right hand revealed hyperkeratosis, intra- and inter-cellular edema, liquefaction, and acanthosis-like 'saw-toothing' of the rete ridges in the epidermis (hematoxylin-eosin stain, original magnification ×100). (c, d, e) There was an inflammatory cell infiltration with some melanophages around capillaries in the upper dermis. Arrows indicate the border of the hyper- (right side) and hypo- (left side) pigmented area (original magnification ×20). (b, d) Fontana–Masson staining showed an increase of melanin-positive cells in both the epidermis and dermis of the hyperpigmented lesion (right side of the arrows); in contrast, no positive cells were seen in the hypopigmented lesion (left side of the arrows) (original magnification ×50 and ×20). (e) Melanocytes with S-100 protein were observed in both the hypopigmented and hyperpigmented areas.

petrolatum was positive after irradiation with half of the UVA-MRD, but not after a half dose of UVB-MED. Two months after the cessation of Preminent®, the patient did not show any response up to 12 J/cm^2 of UVA. Based on these findings, we diagnosed the patient with photoleukomelanoderma. The photosensitivity was most likely caused by hydrochlorothiazide, as there have been only a few reports regarding losartan-induced photosensitivity. Furthermore, no case of photosensitivity due to losartan in Preminent® has been reported so far. Two months after discontinuation of Preminent®, the depigmented lesions improved with topical application of tacrolimus hydrate and hydrocortisone butyrate propionate. At 5-month follow-up, the skin had returned to a normal skin color.

Discussion

Photoleukomelanoderma is a very rare condition with a few reports in the English literature. A limited number of causative drugs have been reported, including thiazide and non-thiazide diuretics, tetracycline, afloqualone, and fenofibrate (2, 3). Photoleukomelanoderma appears to primarily affect Asians (Fitzpatrick skin type II–IV); there have been no cases affecting Caucasians in the literature. In an analysis of 33 European cases of thiazide-induced photosensitivity by Addo *et al.* (4), there were no cases of photoleukomelanoderma. Ishikawa *et al.* (2) hypothesized that Caucasians do not readily suffer from photoleukomelanoderma because they have lower melanization than

Asians. We speculate that leukomelanoderma might be difficult to detect in patients with Fitzpatrick skin types I.

The histological findings of this case suggest that the inflammation may have caused melanocytes in the hypopigmented area to lose some of their functions, such as transport or production of melanin, while activating melanocytes in the hyperpigmented area. Our patient developed leukomelanoderma during a period when there was strong sunshine; the inflammation caused by photosensitivity might have caused excessive damage to melanocytes, leading to a temporary loss of their function. However, the damaged melanocytes are able to survive, unlike the melanocytes in vitiligo, in which the number of melanocytes decreases because of autoimmune dysregulation. The complete recovery in a short period in this case is consistent with our hypothesis.

Photosensitivity because of hydrochlorothiazide has often been reported in the 1980s (4), after which the number of cases decreased with the decrease in prescription of this drug. From 1995, the combination of losartan potassium and hydrochlorothiazide became commercially available as a useful anti-hypertensive drug. Since then, there have been cases of photosensitivity caused by hydrochlorothiazide in anti-hypertensive agents containing an angiotensin II receptor blocker (e.g., losartan potassium) and hydrochlorothiazide (5). To the best of our knowledge, there have been eight case reports of photoleukomelanoderma induced by hydrochlorothiazide; all of them were Japanese patients (5). In five of the six cases, with the exception of the unspecified two cases, leukomelanoderma developed after 1–3 months of further sun exposure following the initial occurrence of photosensitivity. As a result of persistent photosensitivity, the prolonged inflammation might have led to melanocyte dysfunction. Most cases relating to hydrochlorothiazide showed prolonged photosensitivity for at least 1 month after withdrawal of the drug (5). In order to prevent photoleukomelanoderma, we suggest that a timely diagnosis and sun protection are required even after cessation of the causative drug.

References

1. Seishima M, Shibuya Y, Kato G, Watanabe K. Photoleukomelanoderma possibly caused by etretinate in a patient with psoriasis. *Acta Derm Venereol* 2010; **90**: 85–86.
2. Ishikawa T, Kamide R, Niimura M. Photoleukomelanodermatitis (Kobori) induced by afloqualone. *J Dermatol* 1994; **21**: 430–433.
3. Marguery MC, Sayed FE, Rakotondrazafy J *et al.* Photoallergy and photoaggravation induced by fenofibrate: cross-photoreaction and transient light reaction. *Eur J Dermatol* 1995; **5**: 204–207.
4. Addo HA, Ferguson J, Frain-Bell W. Thiazide-induced photosensitivity: a study of 33 subjects. *Br J Dermatol* 1987; **116**: 749–760.
5. Tanaka E, Bito T, Masuoka E *et al.* Six cases of photosensitive disorders possibly due to hydrochlorothiazide. *Skin Research* 2011; **10**: 133–140.

The American Journal of Pathology, Vol. 179, No. 6, December 2011

DOI: 10.1016/j.ajpath.2011.08.042

Tumorigenesis and Neoplastic Progression

Increased Expression of Versican in the Inflammatory Response to UVB- and Reactive Oxygen Species-Induced Skin Tumorigenesis

Makoto Kunisada,* Flandiana Yogianti,* Kunihiko Sakumi,† Ryusuke Ono,* Yusaku Nakabeppu,† and Chikako Nishigori*

From the Division of Dermatology, Department of Internal Related, Kobe University Graduate School of Medicine, Kobe University, Kobe; and the Division of Neurofunctional Genomics,† Medical Institute of Bioregulation, Kyusyu University, Fukuoka, Japan*

Excessive exposure to UV radiation is a major risk factor for developing skin cancer. UV-induced reactive oxygen species (ROS) cause accumulation of DNA damage products such as 8-oxoguanine (8-oxoG) in the skin. We have previously shown that mice lacking the repair enzyme 8-oxoguanine glycosylase (*Ogg1* knockout mice) are highly susceptible to skin cancer after long-term UVB exposure. To investigate the genes involved, we performed gene profiling of *Ogg1* knockout mouse skin after UVB exposure. Among the up-regulated genes in UVB-treated *Ogg1* knockout mice, inflammatory response pathway-related genes were most affected. The Vcan gene, which encodes the large extracellular matrix proteoglycan versican, was continuously up-regulated in UVB-treated *Ogg1* knockout mice, suggesting that versican is a mediator of skin cancer development. We examined the expression pattern of versican in skin tumors from wild-type mice and UVB-treated *Ogg1* knockout mice, and also analyzed 157 sun-related human skin tumors. Versican was strongly expressed in malignant skin tumors in both mice and humans, and especially in *Ogg1* knockout mice. Additionally, infiltrating neutrophils strongly colocalized with versican in UVB-treated *Ogg1* knockout mouse skin. These data demonstrate that inflammatory responses, particularly neutrophil infiltration and versican up-regulation, are closely involved in UVB/ROS-induced skin tumorigenesis. *(Am J Pathol 2011, 179:3056–3065; DOI: 10.1016/j.ajpath.2011.08.042)*

The mechanism of sunlight-induced skin carcinogenesis has been extensively investigated, and direct DNA damage with subsequent generation of dipyrimidine photoproducts has been considered a major cause of skin cancer.[1,2] On the other hand, UV irradiation is known to induce the generation of reactive oxygen species (ROS), which in turn cause various types of DNA damage. Among many oxidative DNA base modifications, 8-oxoguanine (8-oxoG) pairs with adenine as well as cytosine during DNA replication, resulting in GC→TA mutations.[3–5] Accumulation of 8-oxoG has been shown in skin cells after irradiation with UVB (wavelength, 280 to 320 nm).[6] UV-induced 8-oxoG has been recognized as responsible for development of skin cancers in both humans and animals.[7,8]

In mammalian cells, *Ogg1* encodes a DNA glycosylase/apurinic/apyrimidinic (AP) lyase that is responsible for the excision of 8-oxoG from DNA.[9] We showed that *Ogg1* knockout mice exhibit impaired ability to excise 8-oxoG from DNA in epidermal cells after UVB exposure and that *Ogg1* knockout mice develop significantly more skin tumors after long-term UVB irradiation than do wild-type or heterozygous mice.[7] In addition, we found that the ratio and incidence of malignant skin tumors produced by chronic UVB irradiation in *Ogg1* knockout mice is significantly higher and occurs at an earlier age than in wild-type or heterozygous mice. Nonetheless, the mechanisms underlying the highly susceptible phenotype of

Supported entirely by the Global Center of Excellence (GCOE) Program for "Education and Research on Signal Transduction Medicine in the Coming Generation" of Japan's Ministry of Education, Culture, Sports, Science and Technology (M.K. and C.N.) and by Health and Labor Science Research Grants for the Specified Disease Treatment Research Program (C.N.).

Accepted for publication August 22, 2011.

Supplemental material for this article can be found at *http://ajp.amjpathol.org* or at doi: 10.1016/j.ajpath.2011.08.042.

Address reprint requests to Chikako Nishigori, M.D., Ph.D., Division of Dermatology, Clinical Molecular Medicine, Faculty of Medicine Kobe University Graduate School of Medicine, Kobe 650-0017, Japan. E-mail: chikako@med.kobe-u.ac.jp.

Ogg1 knockout mice for developing UVB-induced skin cancers remain to be fully elucidated.

In the present study, we performed gene profiling of UVB-irradiated skin to investigate the relevant genes involved in the susceptibility to skin cancer in *Ogg1* knockout mice. We found that inflammatory pathway-related genes were most significantly affected among the up-regulated genes in *Ogg1* knockout mice. Among the continuously up-regulated genes in *Ogg1* knockout mice after UVB exposure, the expression of Vcan (the gene encoding versican, a large chondroitin sulfate proteoglycan) significantly and persistently differed between wild-type and *Ogg1* knockout mice after UVB exposure. Versican is a component of the extracellular matrix (ECM). It participates in the release of cytokines from the ECM and interacts with other ECM molecules, including collagen, proteoglycans, hyaluronan, and glycoproteins.[10,11] We studied versican expression in skin tumors of wild-type and *Ogg1* knockout mice after long-term UVB exposure, as well as in human sunlight-related skin tumors, and found that strong versican expression is highly associated with UV/ROS-related skin tumors. To study the role of versican in ROS-induced 8-oxoG accumulation, the inflammatory response, and the development of skin tumors, we further assessed the involvement of neutrophil infiltration in UVB-exposed wild-type and *Ogg1* knockout mice.

Materials and Methods

Mice

C57BL/6J *Ogg1* knockout mice[12] and their respective wild-type counterparts were used for gene profiling of the skin and for immunohistochemical studies after UVB exposure. Mice aged 8 to 9 weeks were selected for all studies. We inbred *Ogg1* heterozygous mice (C57BL/6J; $n = 12$), and their genotype was determined as described previously.[12] The mice were housed under special pathogen-free conditions, and all animal experiments were conducted according to the Guidelines for Animal Experimentation of the Kobe University School of Medicine.

RNA Isolation, Gene Expression Profiling, and Real-Time Quantitative PCR

RNAs from skin isolated at each time point were used for microarray and real-time PCR analyses. After genotyping, tissue samples were pooled into two separate groups per genotype for biological replicates. The duplicated RNAs were isolated according to a method described previously,[13] and cyanine 5-labeled cRNAs were generated and hybridized to the CodeLink Mouse Whole Genome Bioarray (35K; Filgen, Nagoya, Japan). Data were analyzed using the Microarray Data Analysis Tool software (version 3.2; Filgen). After screening out weakly labeled genes (ie, those with a weak signal), we analyzed only strongly labeled genes normalized with *GAPDH* levels. Genes with a fold difference of >1.5 or <0.5 were considered significant and were subjected to a validation study, such as real-time quantitative RT-PCR.

To study kinetic gene regulation after UVB exposure, gene clusters were defined with the primary focus on expression at 24 hours after UVB exposure, the time point at which the most significant difference in 8-oxoG formation was observed.[7] The significant genes expressed at 3 and 24 hours after UVB exposure were categorized into six clusters, as follows, in terms of expression at 3 and 24 hours after UVB exposure: up-regulated and up-regulated (cluster 1), not significant and up-regulated (cluster 2), down-regulated and up-regulated (cluster 3), down-regulated and down-regulated (cluster 4), not significant and down-regulated (cluster 5), and up-regulated and down-regulated (cluster 6). Pathway analysis for samples exposed to 24 hours of UVB was performed with Microarray Data Analysis Tool software (version 3.2; Filgen, Nagoya, Japan), which uses GenMAPP (*http://www.genmapp.org*) and WikiPathways (*http://wikipathways.org/index.php/WikiPathways*) databases. Once a group of statistically significant ($P < 0.05$) pathway genes was formed, gene relationships within pathways were visualized with schematic figures obtained from WikiPathways.

Two-step real-time quantitative RT-PCR using Universal ProbeLibrary (LightCycler 480 System II; Roche, Mannheim, Germany) was performed to confirm microarray results. The following genes were analyzed using real-time PCR: *Il1b*, *Vcan*, *Apod*, *Saa3*, *Aif1*, *Fbn1*, *Slit2*, *Mmp2*, *Tnf* (alias *Tnfa*), and *Cxcl1* (alias *KC*). Total RNAs from the back skin of wild-type mice isolated at 24 hours after UVB exposure at 250 mJ/cm^2 were used to generate a standard curve. Each group of RNAs was assayed in duplicate samples by real-time PCR. Expression levels were normalized to those of *GAPDH*. The primers pairs were designed in the hyaluronan-binding region domain encompassing the intron of *Vcan*: 5′-TGGGATTGAAGACACTCAGGA-3′ as a forward primer in exon 3 and 5′-TGGCTGCCCTGTAGTGAAA-3′ as a reverse primer in exon 4.[14] Statistical differences were determined using an unpaired *t*-test for relative mRNA expression analyzed; $P < 0.05$ was considered to be statistically significant.

UVB Irradiation

Banks of six TL 20W/12RS fluorescent lamps (Philips, Eindhoven, Holland) were used to irradiate the mice with broad-band UVB. These lamps emit a continuous spectrum from 275 to 390 nm, with peak emission at 313 nm; approximately 65% of that radiation is within the UVB wavelength range. The irradiance was 3.8 J/m^2 · s for the lamps at a distance of 40 cm, as measured by an UVR-305/365D digital radiometer (Tokyo Optical Company; Tokyo Kogaku Kikai KK, Tokyo, Japan). Before the back skin of mice was taken, the backs of the mice were shaved; the mice were then placed 40 cm below the bank of lamps and were irradiated. For immunohistochemical and immunofluorescence studies, 8-week-old mice were irradiated with UVB at 250 mJ/cm^2, which is the approximate minimal erythema dose for C57BL/6J mice.

Analysis of UV-Induced Murine Skin Tumors and Sun-Related Human Skin Tumors

All skin tumors developed in wild-type and *Ogg1* knockout mice after chronic exposure to UVB were sampled for immunohistochemical analyses. Tumors were induced by irradiation with broadband UVB at the minimal erythema dose three times per week for 40 weeks.[7,15] The histologically examined wild-type samples were squamous cell carcinoma (SCC; $n = 5$), sarcoma ($n = 1$), and papilloma ($n = 5$); the *Ogg1* knockout samples were SCC ($n = 19$), sarcoma ($n = 4$), and papilloma ($n = 3$). Human skin tumor samples were also examined for immunohistochemical analysis. Patient samples previously examined by independent dermatopathologists were selected from the archival tissue sample collection of the Division of Dermatology of the Kobe University of Medicine. We focused primarily on human UV-induced malignant and benign tumors. The tumors selected (except for malignant melanoma, all the tumors had developed on sun-exposed skin areas) were as follows: malignant melanoma ($n = 32$), lentigo maligna melanoma ($n = 11$), superficial spreading melanoma ($n = 7$), acral lentiginous melanoma ($n = 11$), nodular melanoma (n =3), basal cell carcinoma ($n = 30$), SCC ($n = 27$), and actinic keratosis ($n = 25$). In addition, seborrheic keratosis ($n = 25$) and lentigo senilis ($n = 18$) lesions were selected as the benign counterparts.

Histology and Immunohistochemistry

For histological analyses, the back skin from wild-type and *Ogg1* knockout mice, dissected at each time point, was fixed in neutralized 10% formalin and embedded in paraffin. Then, 4-μm sections were cut, deparaffinized, rehydrated, and washed in PBS. Sections placed in 10 mmol/L of citrate buffer (pH 6.0) were microwaved three times for 5 minutes. After blocking of endogenous peroxidase, nonspecific binding sites were blocked by incubating the sections with protein blocking serum (Dako, Kyoto, Japan). Sections were incubated for 16 hours at 4°C with the following primary antibodies: rabbit polyclonal anti-mouse IL-1β (1:1000 dilution; Abcam, Cambridge, MA), rabbit polyclonal anti-mouse versican (1:100 dilution; LifeSpan Biosciences, Seattle, WA), rabbit polyclonal anti-human versican (1:125 dilution; Atlas Antibodies, Stockholm, Sweden), or rabbit polyclonal anti-mouse p53 (CM5) (1:500 dilution; Leica Biosystems Newcastle, Newcastle upon Tyne, UK). The antibody of murine versican that is capable of detecting glycosaminoglycan domain β could identify V0 and V1 isoforms, which have been shown to be functional in cell proliferation and anti-apoptosis.[16] Human versican antibody can be used to detect hyaluronan-binding domain; it was used to detect the V0, V1, V2, and V3 isoforms. After a washing with PBS, the sections were incubated with biotin-conjugated anti-rabbit IgG (IgG; Dako) for 20 minutes at room temperature, followed by incubation for 15 minutes with streptavidin-conjugated horseradish peroxidase (Dako) at room temperature before counterstaining with hematoxylin. Finally, sections were mounted with Glycergel mounting medium (Dako). Samples were analyzed under an all-in-one fluorescence microscope (Biozero BZ-8000; Keyence, Osaka, Japan). For immunofluorescence staining, 4-μm frozen sections were incubated with the rat monoclonal anti-mouse Ly-6G/Gr-1 antibody (1:100 dilution; Pharmingen; BD Biosciences, San Diego, CA) or the rabbit polyclonal anti-mouse versican antibody (1:100 dilution; LifeSpan Biosciences). Then, sections were incubated with Alexa Fluor 488-conjugated secondary antibodies (Invitrogen, Carlsbad, CA) before applying DAPI (Invitrogen). Versican positivity in mouse and human tumors was analyzed and classified as high (>50% of positive cells) or low (≤50%), diagnosed by two independent dermatopathologists (C.N. and R.O.). To quantify the number of neutrophils present in mouse skin samples after UVB exposure, the number of granulocyte receptor-1 (Gr-1)-positive cells detected by immunofluorescence was counted in ten 800-μm^2 areas. The average number of Gr-1-positive cells was then calculated for each genotype.

Statistical differences were determined using an unpaired *t*-test for the number of Gr-1 positive cells analyzed; $P < 0.05$ was considered to be statistically significant.

Western Blot Analysis

Western blotting was performed as described previously.[17] Briefly, 10.0 μg of protein was electrophoresed on 10% sodium dodecylsulfate-polyacrylamide gels and transferred to polyvinylidene difluoride membranes. Membranes were incubated with rabbit polyclonal anti-mouse versican (1:1000 dilution; LifeSpan Biosciences), rabbit polyclonal anti-mouse p53 (CM5) (1:2000 dilution; Leica Biosystems Newcastle), or α/β-tubulin (1:500 dilution; Cell Signaling Technology, Danvers, MA) as loading control, followed by reaction with alkaline phosphatase-linked IgG (Promega, Madison, WI). Immunoreactive bands were visualized after reaction with Nitro Blue Tetrazolium/5-bromo-4-chloro-3′-indole phosphate (NBT/BCIP) solution (Promega).

Results

Time-Course Analysis of Gene Expression in Ogg1 *Knockout Mice after UVB Exposure*

To investigate which genes are up- or down-regulated after UVB irradiation in wild-type and *Ogg1* knockout mice, we performed microarray gene profiling of skin at 3 and 24 hours after exposure. We extracted the significant genes at each time point and sorted the genes with a fold difference of >1.5 or <0.5, after excluding low-intensity signals. This microarray study revealed that 255 genes were up-regulated and 426 genes were down-regulated in *Ogg1* knockout mice at 3 hours after UVB exposure and that 372 and 206 genes were up- and down-regulated at 24 hours after UVB exposure, respectively (Figure 1A). To understand the kinetics of gene regulation

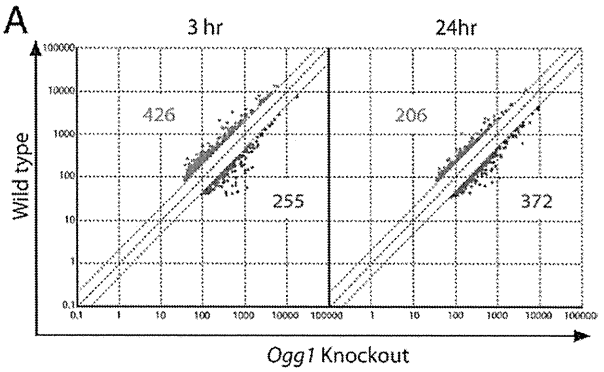

B

Clusters	3 hr	24 hr	Schema	The number of genes
1	Up	Up		22
2	N.S	Up		282
3	Down	Up		68
4	Down	Down		1
5	N.S	Down		184
6	Up	Down		21

Figure 1. Time-course analysis of gene expression in *Ogg1* knockout mouse skin after UVB exposure. **A:** Genes up- or down-regulated at 3 and 24 hours after exposure of *Ogg1* knockout and wild-type mice to UVB. Dots represent genes with an expression difference of >1.5 or <0.5 times (significant genes) after exclusion of low-intensity microarray signals. Red and blue dots represent up- and down-regulated genes in *Ogg1*-knockout, respectively, with the number of up- and down-regulated genes indicated in the corresponding color. **B:** Clusters of up- and down-regulated genes at each time point were categorized based on the trend of up- or down-regulation at 3 and 24 hours after UVB exposure. Schematics are shown for the six clusters, along with the number of genes assigned to each cluster.

after UVB exposure, gene clusters were defined with a primary focus on expression at 24 hours after UVB exposure, at which point the most significant difference in 8-oxoG formation was observed.[7] The main reason for using cluster analysis in the present study was to identify the constitutively up-regulated (down-regulated) genes because we speculated that among those genes, there may be the most probable candidate genes for skin cancers with positive (negative) driving forces by up-regulated (down-regulated) genes. The numbers of significant genes in each cluster at 3 and 24 hours after UVB exposure are presented in Figure 1B. These data were further analyzed in our next study.

The Inflammatory Pathway Is the Most Affected among Up-Regulated Genes at 24 Hours after UVB Exposure

Previously, we have shown by immunohistochemistry that UVB-induced epidermal 8-oxoG accumulation is significantly different between wild-type and *Ogg1* knockout mice at 24 hours, compared with 3 hours, after UVB exposure.[7] First, to elucidate gene regulation in terms of the pathways affected in *Ogg1*-knockout mice after UVB, we performed pathway analysis using the Microarray Data Analysis Tool (GenMAPP and WikiPathways) for 372 up-regulated and 206 down-regulated genes in *Ogg1*-knockout at 24 hours after UVB exposure. We selected significant pathways with high *Z*-score and low *P* value (<0.5). Surprisingly, the inflammatory response pathway was the most significantly affected pathway, with 7 of 39 genes altered (Table 1). The second most significant pathway was the complement and coagulation cascade. We further investigated the significant genes involved in the inflammatory pathway. Those genes included *Il1b*, *Cd80*, *Col1a2*, *Col3a1*, *Fn1*, *Fcgr1*, and *Ighm* (alias *Igh-6*). The pathway involvement of seven genes previously shown to be related to the skin is presented in Figure 2A.

We selected *Il1b*, which is one of the key genes expressed by macrophages, for validation studies. Using real-time quantitative RT-PCR, we confirmed that the expression levels of *Il1b* in *Ogg1* knockout mice at 24 hours after UVB exposure were 7.1-fold higher than in the wild-type counterparts (Figure 2B). Moreover, we studied the expression pattern of IL-1β in the skin of UVB-exposed or control *Ogg1* knockout mice. Expression of IL-1β in the epidermis and dermal cells in *Ogg1* knockout mice was higher than in the wild-type mice. On the other hand, nonirradiated skin was negative for IL-1β (Figure 2C), which is consistent with results from the microarray and real-time PCR analyses.

Versican Is Strongly Up-Regulated in the Skin and in UVB-Induced Tumors of Ogg1 *Knockout Mice*

Accumulation of 8-oxoG in the epidermis at 3 and 24 hours after UVB exposure is higher in *Ogg1* knockout mice than in wild-type mice, implying that the continuously up- or down-regulated genes are involved in skin tumor development in *Ogg1* knockout mice.[7] Next, we focused on constitutively up-regulated (or down-regu-

Table 1. Pathway Analysis for Changes in Gene Expression in *Ogg1*$^{-/-}$ Mice 24 Hours after UVB Exposure

Pathway name*	Total genes (no.)	Changed expression (no.)	*P* value
Increased Expression			
Inflammatory response	39	7	0.000054
Complement/coagulation	56	7	0.00042
Striated muscle contraction	41	5	0.0032
Complement activation (classical pathway)	13	3	0.0049
Decreased Expression			
Hypertrophy model	19	3	0.0015
GPCR (class A, rhodopsin-like)	187	7	0.0035
Id signaling pathway	48	3	0.016
Small ligand GPCRs	19	2	0.020

*Top four pathways involving significantly increased or decreased gene expression, as extracted from microarray data.
GPCR, G protein-coupled receptor.

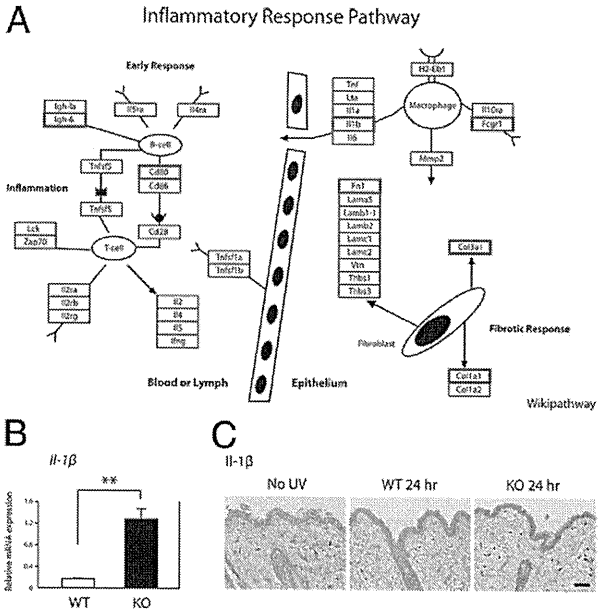

Figure 2. The inflammatory pathway is the most affected among the up-regulated genes at 24 hours after UVB exposure. **A:** The relationships among significantly up-regulated genes involved in inflammatory response pathways in *Ogg1* knockout mice at 24 hours after UVB exposure. Significantly up-regulated genes, previously shown to be involved in skin, were selected from microarray data (**red rectangles**). The schematic figure was modified from WikiPathways (available at *http://www.wikipathways.org/index.php/Pathway:WP458*). **B:** Relative IL-1β gene expression levels in wild-type (WT) and *Ogg1* knockout (KO) mouse skin, as determined by real-time quantitative PCR. Each of the two groups of RNAs isolated from wild-type and *Ogg1* knockout mice was assayed in duplicate. $^{**}P < 0.01$. Data are representative of three separate determinations. **C:** IL-1β gene expression levels in the skin of wild-type and *Ogg1* knockout mice at 24 hours after UVB exposure. Positive signals are seen as reddish-brown deposits produced on reaction with the 3-amino-9-ethylcarbazole substrate. The UVB dose was 250 mJ/cm^2. Weak or no expression of IL-1β is seen in wild-type mouse skin with and without UVB exposure. Scale bar = 30 μm.

lated) genes, because we speculated that some of these genes are the most probable candidate genes for developing skin cancers with correspondingly positive or negative driving forces of the up-regulated or down-regulated) genes. Of note, 22 continuously up-regulated genes (cluster 1) were observed in gene clusters, but only one gene was continuously down-regulated (cluster 4) (Figure 1B). These data suggest that some of the 22 continuously up-regulated genes in UVB-exposed *Ogg1* knockout mice are likely to contribute to skin carcinogenesis. These 22 genes are detailed in Table 2.

We performed validation studies for some of the 22 genes by real-time quantitative RT-PCR. Consistent with the microarray data, the expressions of *Vcan*, *Saa3*, *Fbn1*, and *Slit2* were significantly higher in *Ogg1* knockout mice than in wild-type mice, both at 3 and at 24 hours after UVB exposure (Figure 3A). Again, in agreement with the microarray data, the expression levels of *Apod* and *Aif1* in *Ogg1* knockout mice were nearly twice of those in wild-type mice (see Supplemental Figure S1 at *http://ajp.amjpathol.org*). Of the six genes analyzed by RT-PCR, versican (*Vcan*) expression most significantly differed between the wild-type and knockout mice; knockout levels were 2.9- and 7.2-fold higher than wild-type at 3 and 24 hours after UVB exposure, respectively. Versican is widely expressed in the skin[18] and has been implicated in a wide variety of biological functions during tumorigenesis.[11,19,20] We therefore focused on versican to further dissect the UVB-induced skin carcinogenic phenotype of *Ogg1* knockout mice.

To determine the expression pattern of versican in the skin after UVB exposure, we performed immunohistochemical staining for versican on the skin of control and UVB-irradiated (24 hours) wild-type and *Ogg1* knockout mice. In wild-type mice, versican was strongly expressed in the epidermis after UVB exposure, but was barely expressed in nonexposed skin (Figure 3B). On the other hand, versican expression was markedly stronger in *Ogg1* knockout mice at 24 hours after UVB exposure than the wild-type counterparts; this strong expression was observed not only in the epidermis but also in some dermal components, such as fibroblasts (Figure 3B). We also performed Western blot analysis for versican of the wild-type and *Ogg1* knockout mouse skin after UVB exposure and found that versican was more up-regulated in the knockout mice than in the wild-type mice at both 24

Table 2. Increased Expression of 22 Genes in *Ogg1*$^{-/-}$ Mice at 3 and 24 Hours after UVB Exposure

	Gene symbol	Gene name
1	*Bst2*	Bone marrow stromal cell antigen 2
2	*Cfb*	Complement factor B
3	*Cxcl13*	Chemokine (C-X-C motif) ligand 13
4	*Apod*	Apolipoprotein D
5		*Mus musculus* hemoglobin Y, beta-like embryonic chain (Hbb-y), mRNA
6	*Ms4a6c*	Membrane-spanning 4-domains, subfamily A, member 6C
7		*Mus musculus* Fc receptor-like protein 2 immunoglobulin short Isoform (Fcrh2) mRNA, complete cds
8		Maa26e10.y1 NCI_CGAP_Li10 Mus musculus cDNA clone IMAGE:3812083 5
9	*Tyrobp*	TYRO protein tyrosine kinase binding protein
10	*Vcan*	Versican
11	*Saa3*	Serum amyloid A 3
12	*9530053H05Rik*	RIKEN cDNA 9530053H05 gene
13	*Aif1*	Allograft inflammatory factor 1
14		*Mus musculus* retinoic acid receptor responder (tazarotene induced) 2 (Rarres2), mRNA
15	*Fcer1g*	Fc receptor, IgE, high affinity 1, gamma polypeptide
16		BY765147 RIKEN full-length enriched, activated spleen Mus musculus cDNA clone F830013C14 3-, mRNA sequence
17	*Pth1r*	Parathyroid hormone 1 receptor
18	*Fbn1*	Fibrillin 1
19	*Slit2*	Slit homolog 2 (Drosophila)
20	*Gpx7*	Glutathione peroxidase 7
21	*Cpxm1*	Carboxypeptidase X 1 (M14 family)
22	*Pf4*	Platelet factor 4

Increased expression was determined on the basis of a ratio of *Ogg1* wild-type to knockout being >2.0, as determined from the microarray data at each time point.

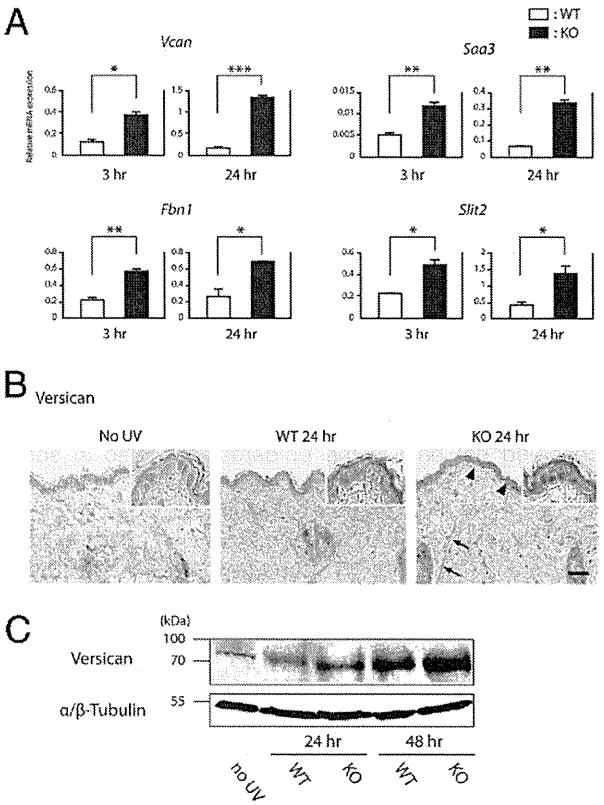

Figure 3. Expression of continuously up-regulated genes after UVB exposure. **A:** Four genes were significantly up-regulated at both 3 and 24 hours after UVB exposure. Relative expression levels were determined by real-time quantitative PCR. Each of the two groups of RNAs isolated from wild-type and *Ogg1* knockout mice was assayed in duplicate. Reactions were normalized to *GAPDH* expression levels. $^{*}P < 0.05$; $^{**}P < 0.01$; and $^{***}P < 0.001$. **B:** Immunohistochemical study of versican expression after UVB irradiation. Versican is barely expressed in the wild-type mouse epidermis and dermis in the absence of UVB irradiation. At 24 hours after UVB exposure, versican was expressed in the wild-type epidermis. In *Ogg1* knockout mice at 24 hours, versican was strongly expressed in the epidermis (**arrowheads**), as well as in dermal fibroblasts (**arrows**). Positive signals are seen as reddish-brown deposits produced on reaction with the 3-amino-9-ethylcarbazole substrate. Scale bar = 30 μm. **C:** Versican expression after UVB exposure, as determined by Western blotting. Versican was more strongly up-regulated in *Ogg1* knockout than in wild-type mice at 24 and 48 hours after UVB exposure. This up-regulation was time-dependent. The band at approximately 75 kDa indicates that the antibody for versican can detect the V1 isoform. α/β-Tubulin was used as the loading control. Data are representative of three separate determinations.

and 48 hours after UVB exposure. In addition, we found that the expression levels of versican indicating V1 isoform were up-regulated in a time-dependent manner (Figure 3C).

Versican Is Strongly Expressed in Skin Tumors Induced in Ogg1 *Knockout Mice after Long-Term UVB Exposure*

We found that high versican expression after single UVB irradiation is associated with *Ogg1* gene disruption. We then investigated whether differences in versican expression between wild-type and *Ogg1* knockout mice can also be found in skin tumors induced by long-term UVB irradiation. We irradiated wild-type and *Ogg1* knockout mice with UVB for more than 40 weeks and obtained 11 tumors in the wild-type mice and 26 tumors in the knockout mice; we diagnosed these tumors histologically as SCC, sarcoma, and papilloma.[7] We performed immunohistochemical staining for versican in all these tumors. Versican was expressed in 17 of 19 SCCs in the knockout mice and in 2 of 5 SCCs in the wild-type mice (Figure 4). All the sarcomas (one in the wild-type and four in the knockout mice) were strongly positive for versican. However, only one of five papillomas in the wild-type and one of three papillomas in the knockout mice were highly positive for versican ($P < 0.05$ for the ratio of malignant tumor/analyzed total tumors of each genotype). Thus, versican was more highly expressed in *Ogg1* knockout mouse tumors than in the wild type. In conclusion, versican expression is especially evident in malignant tumors, compared with benign skin tumors.

Versican Is Expressed in Various Sun-Related Human Skin Tumors

To further examine versican expression, we investigated whether versican is expressed in human skin tumors associated with long-term UV exposure. We performed immunohistochemistry in 157 human skin tumors. We selected tumors that had developed on sun-exposed areas of the skin (the exception being malignant melanoma). Strong versican expression was seen mostly in the dermis and in the stromal components around the tumors, rather than in the tumor cells (Figure 5, A and B). This observation was more evident in malignant than in benign tumors. Basal cell carcinoma, for instance, was positive for versican in 80% (24/30) of the analyzed tumors; expression was noted in stromal areas around the tumor cells (Figure 5A). Lentigo maligna melanoma, a malignant melanoma that usually develops on chronically sun-exposed areas, revealed strong versican expression in the dermis of 8 of 11 tumors. The other three malignant melanoma types showed milder versican expression. These data suggest that lentigo maligna melanoma might be strongly associated with UV/ROS-induced 8-oxoG formation and that it might be of different etiology as opposed to the other malignant mela-

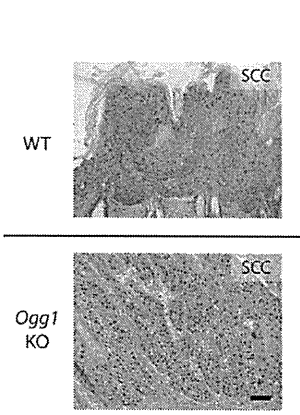

		High Expression	Low Expression	Total Analyzed
WT	SCC	2	3	5
	Sarcoma	1	0	1
	Papilloma	1	4	5
	Total (%)	4 (36.4)*	7 (63.4)	11 (100)
Ogg1 KO	SCC	17	2	19
	Sarcoma	4	0	4
	Papilloma	1	2	3
	Total (%)	22 (84.6)*	4 (15.4)	26 (100)

Figure 4. Versican expression in developing skin tumors of chronically UVB-exposed mice. Representative histological sections of SCC tumors from wild-type and *Ogg1* knockout mice red-colored staining positively for versican are shown, with a summary of versican-positive wild-type and *Ogg1* knockout mouse tumors overall. $^{*}P < 0.05$ for the ratio of malignant tumor to total tumors analyzed for each genotype.

A

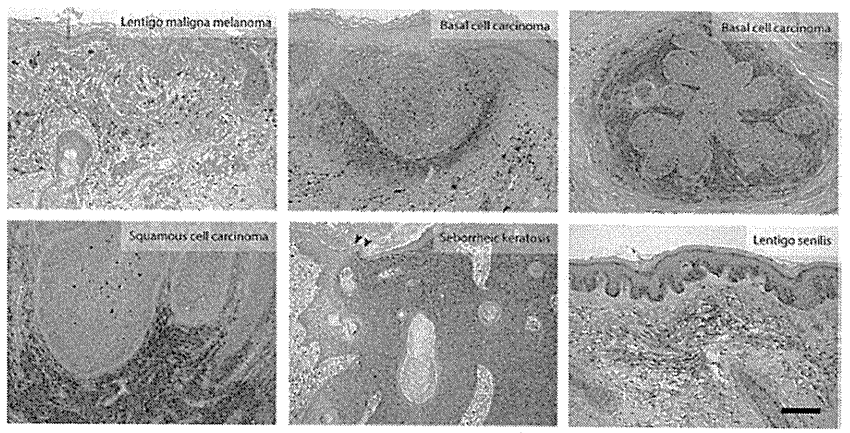

B

Human skin tumors	The number of Patients	Versican expression			
		Dermal and stromal components		Tumor cells	
		High Expression	Low Expression	High Expression	Low Expression
Malignant	114	51	63	11	103
Malignant melanoma	32	9	23	4	28
Lentigo maligna melanoma	11	7	4	2	9
Superficial spreading melanoma	7	1	6	1	6
Acral lentiginous melanoma	11	1	10	1	10
Nodular melanoma	3	0	3	0	3
Basal cell carcinoma	30	22	8	6	24
Squamous cell carcinoma	27	15	12	1	26
Actinic keratosis	25	5	20	0	25
Benign	43	14	29	3	40
Seborrheic keratosis	25	6	19	3	22
Lentigo senilis	18	8	10	0	18

Figure 5. Versican expression in human skin tumors. **A:** Immunohistochemical study of versican expression in malignant (lentigo maligna melanoma, basal cell carcinoma, and squamous cell carcinoma) and benign (seborrheic keratosis and lentigo senilis) tumors. **Arrowheads** indicate the borders between the seborrheic keratosis tumor and the normal skin. Scale bar = 100 μm. **B:** Classification of versican expression in skin tumors, grouped as dermal and stromal versus tumoral.

noma types. Although versican expression was relatively weaker in benign tumors than in malignant skin tumors, some tumors, such as seborrheic keratosis, showed stronger expression in tumor cells than in the dermis around the tumors (Figure 5, A and B).

High Versican Expression Is Accompanied by Inflammatory Neutrophil Infiltration

Finally, we investigated the mechanisms associated with UVB-induced high versican expression in *Ogg1* knockout mice. Notably, we found that most human malignant and benign tumors with high versican expression were enriched with inflammatory cells in the tumors or in the dermis around them (Figure 6A). Versican was highly expressed both in inflammatory cells, especially segmented leukocytes (neutrophils), and in the dermal component. To ascertain whether dermal neutrophils interact with versican, we performed immunofluorescence double staining for versican and the neutrophil marker Gr-1. We irradiated wild-type mice with a single minimal erythema dose of UVB and dissected the skin after 24 hours. Gr-1 and versican were colocalized in infiltrated neutrophils, indicating that UVB-induced skin neutrophils interact with versican (Figure 6B). The interaction between versican and neutrophils suggests that the amount of neutrophils differs between wild-type and *Ogg1* knockout mice. Indeed, when we compared the number of neutrophils infiltrated in the dermis at 24 and 48 hours after UVB exposure between wild-type and *Ogg1* knockout mice,[20] the number of neutrophils was significantly increased in *Ogg1* knockout mice, compared with the wild-type mice (Figure 6C). Taken together, high versican expression in *Ogg1* knockout mouse skin after UVB exposure is highly associated with the inflammatory response, particularly neutrophil infiltration (Figure 7).

Discussion

Gene Profiling of UVB-Irradiated Ogg1 *Knockout Mice*

UV rays induce ROS formation, which provoke DNA damage in the skin and subsequent formation of DNA damage products, such as 8-oxoG.[6] Previously, we have shown that *Ogg1* knockout mice exhibit a highly carcinogenic phenotype, with more early-induced malignant skin